Detection of Coronavirus RNA and Antigen in Multiple Sclerosis Brain

Ronald S. Murray, MD,* Bonnie Brown, BS,* David Brian, PhD, DVM,† and Gary F. Cabirac, PhD*‡

Epidemiological studies of patients with multiple sclerosis (MS) and animal model data support the hypothesis that viruses initiate the immunopathogenic events leading to demyelination in MS. There have been no reports, however, of consistent detection of viruses in MS central nervous system tissue. We probed MS and control brain with cDNA probes specific for human, murine, porcine, and bovine coronaviruses. We report the in situ hybridization detection of coronavirus RNA in 12 of 22 MS brain samples using cloned coronavirus cDNA probes. In addition, tissue was screened for coronavirus antigen by immunohistochemical methods; antigen was detected in two patients with rapidly progressive MS. Significant amounts of coronavirus antigen and RNA were observed in active demyelinating plaques from these two patients. These findings show that coronaviruses can infect the human central nervous system and raise the possibility that these viruses may contribute to the pathogenesis of MS in some patients.

Murray RS, Brown B, Brian D, Cabirac GF. Detection of coronavirus RNA and antigen in multiple sclerosis brain. Ann Neurol 1992;31:525–533

Multiple sclerosis (MS) is a chronic inflammatory demyelinating disease of the human central nervous system (CNS) without known cause. A popular theory proposes that an exogenous stimulus initiates an immune response against endogenous CNS proteins, possibly myelin structural proteins. However, damage to the CNS as the result of an immune response to a chronic low-grade CNS infection has never been ruled out. Therefore, demyelinating lesions in MS may represent the final direct or indirect immunopathological reaction to an infectious agent. Supporting this hypothesis are epidemiological studies that strongly implicate an environmental factor in the development of MS [1]. Particularly compelling are the MS epidemic in the Faroe Islands [2] and the recent study of offspring of immigrants to the United Kingdom from low-incidence countries in whom MS developed at rates similar to the indigenous English population [3].

Several common human RNA or DNA viruses have been implicated in the pathogenesis of MS, but none have been definitively associated with the disease [4]. We have been unsuccessful in detecting herpes simplex virus (HSV) type I, cytomegalovirus, varicella zoster virus, Epstein-Barr virus or *Borrelia burgdorferi* (unpublished data), human T-cell lymphotropic virus [5, 6], or measles, mumps, and rubella viruses (Godec MS. Unpublished observations, 1992) in MS brain by in situ hybridization, immunohistochemistry, or polymerase chain reaction.

Coronaviruses have been implicated in MS as a result of the report of virus isolation from the brains of two patients with MS and the electron microscopic observation of a coronavirus in an MS brain perivascular immunocyte [7, 8]. Support for the idea that coronaviruses have a role in MS comes from data showing that these viruses cause demyelination [9] and are capable of stimulating T-cell–mediated autoimmune reactions in rodents [10, 11]. Although these studies are intriguing, more evidence is needed to confirm that coronaviruses infect the human CNS before an association between this type of virus and MS can be made. Because direct coronavirus isolation from human CNS tissue is difficult and fraught with questions concerning isolate origin, we used in situ nucleic acid hybridization and immunohistochemistry to probe for coronavirus RNA and antigen, respectively, in MS and control tissue. We report the detection of coronavirus RNA sequences in brain and, most important, the presence of coronavirus RNA and antigen in demyelinating lesions.

Materials and Methods

Experimental Design

The problem of sampling error of MS brain is significant because the ratio of active-to-inactive lesions is low in patients autopsied after years of disease. Difficulties in detecting and isolating a pathogen arise primarily from the efficiency with which the immune system works. In models of viral

From the *Rocky Mountain Multiple Sclerosis Center, Colorado Neurological Institute, and Swedish Medical Center, Englewood, CO; the †Department of Microbiology, University of Tennessee, Knoxville, TN; and the ‡Department of Biochemistry, Biophysics and Genetics, University of Colorado Health Sciences Center, Denver, CO.

Received Oct 30, 1991, and in revised form Jan 24 and Feb 11, 1992. Accepted for publication Feb 12, 1992.

Address correspondence to Dr Murray, Rocky Mountain Multiple Sclerosis Center, Dept 7500LB, 501 East Hampden Ave, Englewood, CO 80110.

pathogenesis, the area of acute early inflammation is most likely to yield positive results because older lesions may have been cleared of the inciting agent. Therefore, we initially screened multiple white matter plaque and nonplaque regions by in situ hybridization using randomly primed ^{35}S-labeled complement DNA (cDNA) probes derived from genomic coronavirus RNA. Total genomic probes increase the likelihood of detection of closely-related coronaviruses. All coronavirus-positive tissue sections and selected control specimens were then further analyzed by in situ hybridization using all cloned cDNA probes specific for the prototypic coronaviruses from two of the three major coronavirus groups. Noncoronavirus probes were used as well to control for nonspecificity of the hybridization procedure. In each probe experiment, subjacent sections were used from the positive tissue block. In addition, coronavirus-specific polyclonal and monoclonal antisera were used to probe for virus antigen by immunohistochemistry in subjacent sections.

Tissue

CNS tissue from 22 patients with MS, 16 control patients with non-neurological disease, and 5 control patients with other neurological diseases was examined. The other neurological diseases included one each of the following: amyotrophic lateral sclerosis, postinfectious encephalomyelitis, bacterial meningitis, subacute sclerosing panencephalitis, and radiation-induced cerebral vasculitis. All tissues were rapidly frozen and stored at −80°C. Average duration from patient death to tissue acquisition and freezing (autolysis time) for MS and control patients was 5.0 and 6.1 hours, respectively.

Histology

Where indicated, histochemical stains were performed according to standard methods for hematoxylin and eosin, oil red O, and luxol-fast blue/periodic acid-Schiff. Oil red O positivity indicates myelin sheath breakdown products in phagocytes by staining esterified cholesterol red; Luxol-fast blue stains intact undigested myelin blue.

Cells and Virus

Delayed brain tumor (DBT) and baby hamster kidney cells (BHK21) were maintained in Dulbecco's modified Eagle medium (Gibco) containing 2% fetal bovine serum, penicillin, and streptomycin. Infection of DBT cell monolayers with either mouse hepatitis virus strain A59 (MHV A59) or coronavirus SD [7] or BHK21 monolayers with the WW strain of Theiler's murine encephalomyelitis virus (TMEV) was as previously described [12, 13]. HeLa cells were infected with HSV-I (F strain) at a multiplicity of infection of 0.1 and incubated at 37°C for 12 hours. Infected or uninfected cells were cytospun onto slides and fixed with either 4% buffered paraformaldehyde, acetone, or ethanol/acetic acid.

In Situ Hybridization

^{35}S-labeled cDNA probe was prepared by reverse transcription of purified viral coronavirus SD or TMEV RNA [13]. The specific activity of these probes was approximately 1×10^8 cpm/μg. Specificity of the probes was confirmed by in situ hybridization to coronavirus SD–infected or –uninfected DBT cells and TMEV–infected or –uninfected BHK21 cells. Positive hybridization to infected cells was abolished by pretreating the infected cells with ribonuclease A (RNase). In situ hybridization was performed as previously described [14]. Briefly, 4-μm-thick frozen sections of MS and control brains were placed onto pretreated slides, fixed with 3:1 v/v ethanol/acetic acid solution, dehydrated through graded alcohols, and pretreated to improve probe diffusion. The hybridization mixture contained 0.6 M NaCl, 50% formamide, 10% dextran sulphate, 1 × Denhardt's solution, 100 μg/mL denatured human nucleic acids, and ^{35}S-labeled probe. Probe concentration was adjusted to 1 ng/20 μL. Hybridization was at room temperature for 72 hours. Following hybridization, sections were washed in 50% formamide, 10 mM Tris (pH, 7.2), and 1 mM EDTA, with manipulations of the salt concentration and temperature as follows: 0.3 M NaCl for 15 minutes at 45°C, then with 0.1 M NaCl for 1 hour at 55°C, then with 0.6 M NaCl for 48 hours at room temperature. Sections were then dehydrated in graded alcohols containing 0.3 M ammonium acetate, air dried, coated with NTB-2 photographic emulsion (Eastman-Kodak Co, Rochester, NY), air dried, and placed in a desiccated container at 4°C. Slides were developed 14 to 21 days later and counterstained with hematoxylin and eosin. Positivity was determined by finding a significant number of silver grains developed over cells compared with background. Microscopic examination of slides was done with both brightfield and darkfield optics. Some sections subjacent to positive sections were pretreated with RNase prior to hybridization to demonstrate that hybridization was attributable to specific RNA.

Following analysis with the ^{35}S-labeled probes as described, ^{32}P-labeled cDNA clones were used for in situ hybridization. We found that ^{32}P-labeled probes decreased emulsion exposure times to a maximum of 5 days. Clones G344, L8, A3, MN3, and FG5 contain cDNA from MHV A59, human coronaviruses 229E and OC43 (HCV 229E and HCV OC43), bovine coronavirus (BCV), and porcine transmissible gastroenteritis coronavirus (TGEV), respectively [15–19]. Clone G344 (insert size, 1.8 kb) contains approximately 200 base pairs (bp) of gene 4, all of genes 5 and 6, and approximately 200 bp of gene 7. Clone L8 (insert size, 1.2 kb) contains only gene 7 sequences. Clones A3, MN3, and FG5 (insert sizes, 1.7, 2.1, and 2.0 kb, respectively) all extend from the 3′ end of gene 6, through gene 7, to the 3′ end of the genome. Clone SD1001, isolated in this laboratory, was obtained from a cDNA library derived from messenger RNA (mRNA) extracted from coronavirus SD–infected DBT cells. Dideoxy sequencing showed that the insert in this clone was 298 bp in length, with 97% sequence identity to the 3′ end of gene 7 and the 3′ untranslated region of MHV JHM (unpublished data). Clone pIGA15 contains the HSV-I ICP0 gene [20]. Inserts were excised from plasmids, purified by gel electrophoresis, labeled with ^{32}P dATP by the random primer method [21], and desalted on Bio-Gel P6 columns (BioRad). Specific activities of the labeled DNAs were 1 to 4×10^9 cpm/μg. Specificity of all probes was confirmed by hybridization to infected and uninfected cells. In situ hybridization was as described except for the following changes in stringency: hybridization was at 42°C for 24 hours; slides were washed at 37°C for 48 hours with 50% formamide, 10 mM Tris (pH, 7.2), 1 mM EDTA, and 0.6 M NaCl; and emulsion was developed after 3 to 5 exposure

days. Sections subjacent to positive tissue sections were hybridized with TMEV cDNA and cloned HSV-I DNA as described for the coronavirus probes or pretreated with RNase prior to hybridization with the coronavirus probes. Other tissues were carried through the in situ hybridization procedure without probe to control for specific silver grain development in the emulsion.

Immunohistochemistry

Four-micron-thick frozen sections were fixed in ethanol/acetic acid (3:1), acetone, or 4% paraformaldehyde, then dehydrated and stored at room temperature. Prior to staining, the sections were rehydrated in phosphate-buffered saline (PBS) for 3 minutes. Sections were incubated sequentially at room temperature with the following reagents at the appropriate dilutions for the time shown and rinsed in PBS after each incubation: (1) normal rabbit serum or normal mouse serum, depending on the species of the primary antisera, 20 minutes; (2) rabbit polyclonal antiserum to coronavirus A59 [22], or mouse monoclonal antibody (mAb J.3.1) to MHV JHM [23], 20 minutes; (3) goat anti-rabbit immunoglobulin G (IgG) or anti-mouse IgG antibody conjugated to horseradish peroxidase, 20 minutes; and (4) 0.5% 3,3-diaminobenzidine in 0.01% H_2O_2 in PBS, 5 minutes. Sections were rinsed in distilled water, blued in 3% copper sulfate for 5 minutes, and counterstained with Gill's hematoxylin. Positive controls were infected tissue culture cells as described. Negative controls included uninfected cells stained as described, or tissue sections or infected cells stained omitting the primary or secondary antibody or the chromophore. The tissue sections used for this negative control staining were sections subjacent to positive sections. In addition, preincubation with rabbit anti-MHV A59 before the addition of murine mAb J.3.1 prevented specific staining in infected cells and positive tissue sections when the secondary antibody was anti-mouse-horseradish peroxidase.

Results

Detection of Coronavirus RNA in the CNS

In the initial screen using ^{35}S-labeled cDNA probes prepared from coronavirus genome, coronavirus RNA was detected in the CNS from 11 of 21 patients with MS (52%) and 2 of 21 patients without MS (9.5%). Significance was determined by chi square ($\chi^2 = 9.02$, 1 degree of freedom, $p < 0.005$). Specifically, coronavirus RNA was detected in CNS tissue from 1 of 16 (6%) patients with non-neurological disease and in 1 of 5 (20%) with other neurological diseases. The other patient with neurological disease positive for coronavirus RNA had radiation-induced cerebral vasculitis. The positive patients with non-neurological and other neurological diseases were both found to have coronavirus RNA in frontal cortex. Although coronavirus RNA was detected in 52% of patients with MS, the number of sections that were positive was relatively low. Only 49 of 442 (11.1%) probed sections from patients with MS contained coronavirus RNA. Coronavirus RNA was identified in both plaque and nonplaque areas of cortex, brainstem, and spinal cord. In general, coronavirus-positive cells (probably glial) found by this screen were few in number yet consistent in subjacent sections. Positive signal was found in only 3 of 376 (0.8%) white matter sections examined from the 21 control patients. CNS tissue from both patients with MS from which coronavirus SD and coronavirus SK were originally isolated [7] were found to be positive for coronavirus RNA. Tissues probed with the TMEV cDNA or HSV probes were negative. Pretreatment of positive control coronavirus–infected cells or sections subjacent to coronavirus RNA–positive CNS sections with RNase eliminated the hybridization signal.

Coronavirus Specificity in Human CNS

Following hybridization with the ^{35}S-labeled genomic cDNA probes, we repeated the experiments on the positive (11 MS and 2 control) patient samples using ^{32}P-labeled cloned coronavirus cDNA. An additional patient with MS with very acute and severe disease and 9 non-MS control patients previously used in the original screen were probed. The cloned cDNAs, representing full or partial nucleocapsid genes, of MHV A59, coronavirus SD, HCV 229E, HCV OC43, BCV, and TGEV are described in the Materials and Methods section. The results are summarized in the Table. All 12 MS patient samples had detectable signal with the MHV A59 and coronavirus SD probes; sections subjacent to these positive sections were also positive with the HCV OC43 probe for 5 of 12 patients. The grain density over positive cells in these 5 patient samples was lower than that seen in the corresponding regions positive with the MHV A59 or coronavirus SD probes. All of these tissues were negative for BCV, TGEV, and HCV 229E. No detectable signal was seen for the 11 control CNS tissues with any of the probes. These 11 control specimens included the two patient samples that were positive in the initial screen. MS and control sections were negative for HSV and TMEV. As stated, RNase pretreatment of subjacent sections of any positive tissue resulted in a loss of hybridization signal. The distribution and localization of coronavirus RNA in tissues detected with these cloned cDNA probes was similar to the results obtained with the total genomic probe. In two patients with rapidly progressive MS, an abundant amount of coronavirus RNA was found in active demyelinating plaques.

Presence of Coronavirus RNA and Antigen in Active Demyelinating Plaques

In two patients with rapidly progressive MS of recent onset, an abundance of coronavirus RNA and antigen was found in active demyelinating plaques (Figs 1, 2). These were the only two patients in which antigen was detected. Active demyelination was determined by the absence of cells containing luxol-fast blue (blue color)

In Situ Hybridization and Immunohistochemical Results

	In Situ Hybridization Probes								Anti-serum				
	MHV A59	SD 1001	HCV OC43	BCV	HCV 229E	TGEV	HSV	TMEV[a]	MHV A59	TMEV	mAb J.3.1	Normal Rabbit	Normal Mouse
MS patients	12/12	12/12	5/12	0/12	0/12	0/12	0/12	0/12	2/12	0/12	2/12	0/12	0/12
Control subjects	0/11	0/11	0/11	0/11	0/11	0/11	0/11	0/11	0/11	0/11	0/11	0/11	0/11
A59–infected cells	+ + +	+ + +	+	. . .	. . .	. . .	. . .	. . .	+ + +	. . .	+ + +	. . .	. . .
SD–infected cells	+ + +	+ + +	+	. . .	. . .	. . .	. . .	. . .	+ + +	. . .	+ + +	. . .	. . .
Uninfected cells	. . .	. . .	. . .	. . .	. . .	. . .	. . .	. . .	. . .	. . .	. . .	. . .	. . .
TMEV–infected cells	. . .	. . .	. . .	. . .	. . .	. . .	. . .	+ + +	. . .	+ + +	. . .	. . .	. . .
HSV–infected cells	. . .	. . .	. . .	. . .	. . .	. . .	+ + +	. . .	ND	ND	ND	ND	ND

[a]cDNA probe derived from TMEV genome RNA; all other probes are cloned cDNA or DNA.

MHV A59 = mouse hepatitis virus strain A59; HCV = human coronavirus; BCV = bovine coronavirus; TGEV = bovine transmissible gastroenteritis coronavirus; HSV = herpes simplex virus type I; TMEV = Theiler's murine encephalomyelitis virus; + + + = very strong signal; + = weak signal; ND = not done.

or oil red O (red color)–positive lipids. Positive hybridization was significant in perivascular cells and cells throughout the plaque that appeared to be lipid-filled macrophages. As stated, coronavirus RNA was detected with probes specific for MHV A59, coronavirus SD, and MHV OC43, but not with the other coronavirus cloned probes, or the TMEV and HSV probes.

Although cell-specific markers were not used, many of the coronavirus RNA–positive cells appeared to be foamy macrophages; these cells stained red with oil red O (see Fig 2). Oil red O stains esterified or digested lipids red, which are prominent in macrophages active in demyelinating plaques. Whether coronavirus RNA was present in glial cells could not be determined, but grey matter regions were consistently negative.

Coronavirus antigen was also detected using monoclonal or polyclonal MHV A59 antisera. Coronavirus antigen was detected in cells that appeared similar to those containing coronavirus RNA (see Fig 2). The mAb J.3.1 is specific for an epitope on the nucleocapsid protein of MHV JHM and cross reacts with the nucleocapsid protein of MHV A59 but not HCV OC43 [23, 24]. As shown in Figure 2, specific binding of this mAb could be blocked by pretreating with polyclonal antisera to MHV A59.

Discussion

Despite the intensive investigations of neurotropic coronaviruses in rodents, human neurological disease resulting from coronavirus infection has not been proved. However, accumulating data suggest that coronaviruses may infect human CNS tissue and that these viruses may differ from the prototypical upper respiratory human coronaviruses [7, 22, 23, 25–27]. The results presented herein support the contention that coronaviruses are capable of infecting human CNS. Surprisingly, of the 12 positive patient samples identified with the murine-specific in situ probe, only 5 were positive with the HCV OC43 probe. In addition, the murine-specific probe produced stronger hybridization signal in these 5 samples compared to the HCV OC43 probe. This finding suggests that the coronavirus detected in MS tissue may be more closely related to the prototypical murine coronavirus in the 3′ end of the genome, or it may be a human-murine recombinant coronavirus.

The fact that the 5 HCV OC43–positive samples were not positive with the BCV probe was unex-

Fig 1. Representative results of in situ hybridization with ^{32}P-labeled cloned probes specific for mouse hepatitis virus strain A59. Similar results were obtained for ^{32}P-labeled probes specific for coronavirus SD. Emulsions were developed after 72 hours of exposure followed by counterstaining of the sections with hematoxylin and eosin. Brightfield and corresponding darkfield photomicrographs are A and D; B and E; C and F; G and J; and H and K. Silver grains are black by brightfield and white by darkfield. (A, D) Perivenular infiltrate of foamy cells most likely representing macrophages are laden with silver grains. (B, E) Field adjacent to A and D within a well-demarcated area of active demyelination showing coronavirus RNA in foamy cells. (C, F) Field outside of plaque region within grey matter showing absence of hybridization. (G, J) A subjacent section to A and D pretreated with ribonuclease A (RNase) obliterates probe hybridization. (H, K) A different patient with a similar pattern of coronavirus RNA detection in foamy-appearing cells in a perivenular area of active demyelination. (I) Delayed brain tumor cells infected with coronavirus SD demonstrating positive hybridization. (L) Same as (I), except cells were pretreated with RNase, with resultant loss of hybridization signal. (All ×400.)

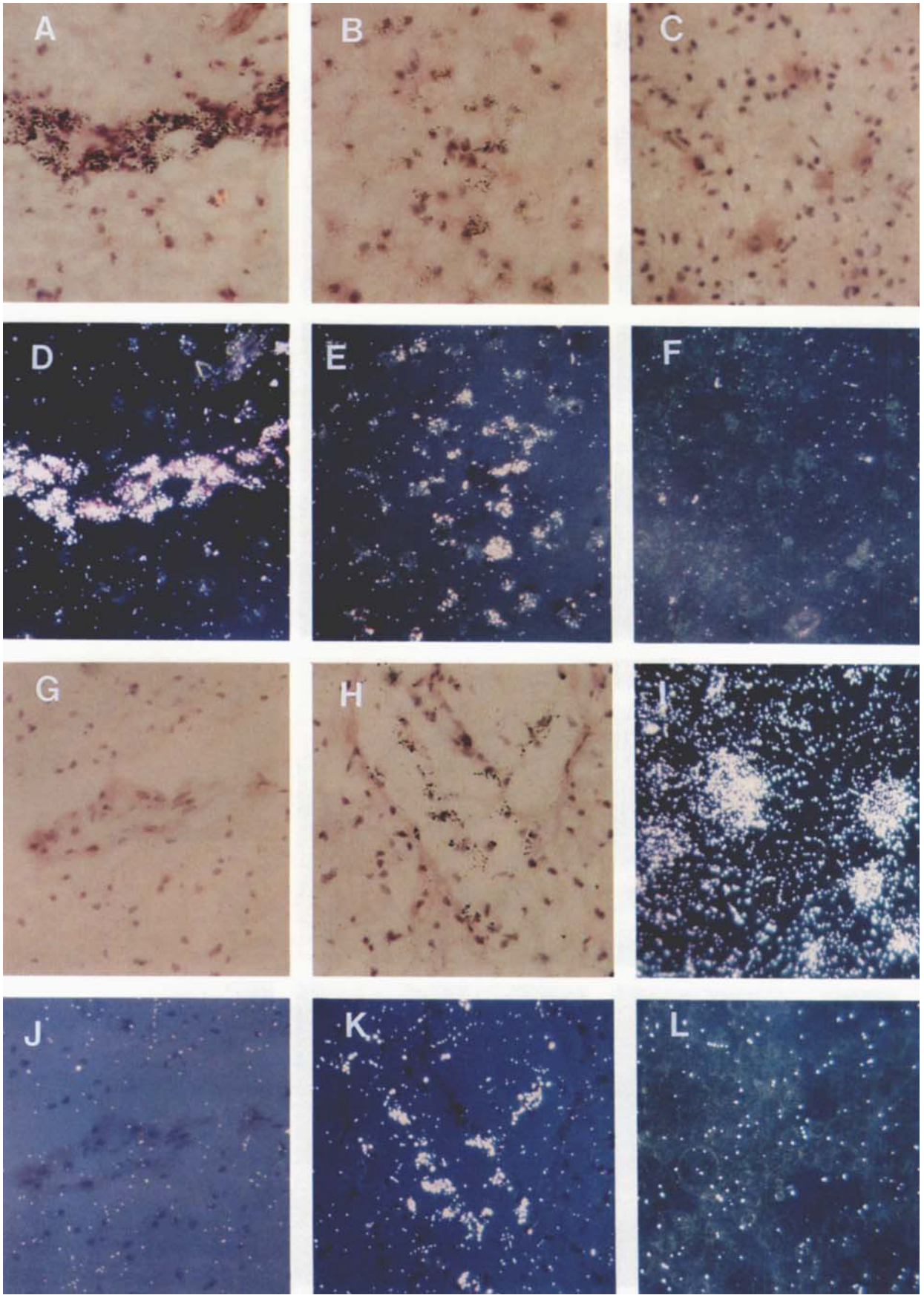
A
B
C
D
E
F
G
H
I
J
K
L

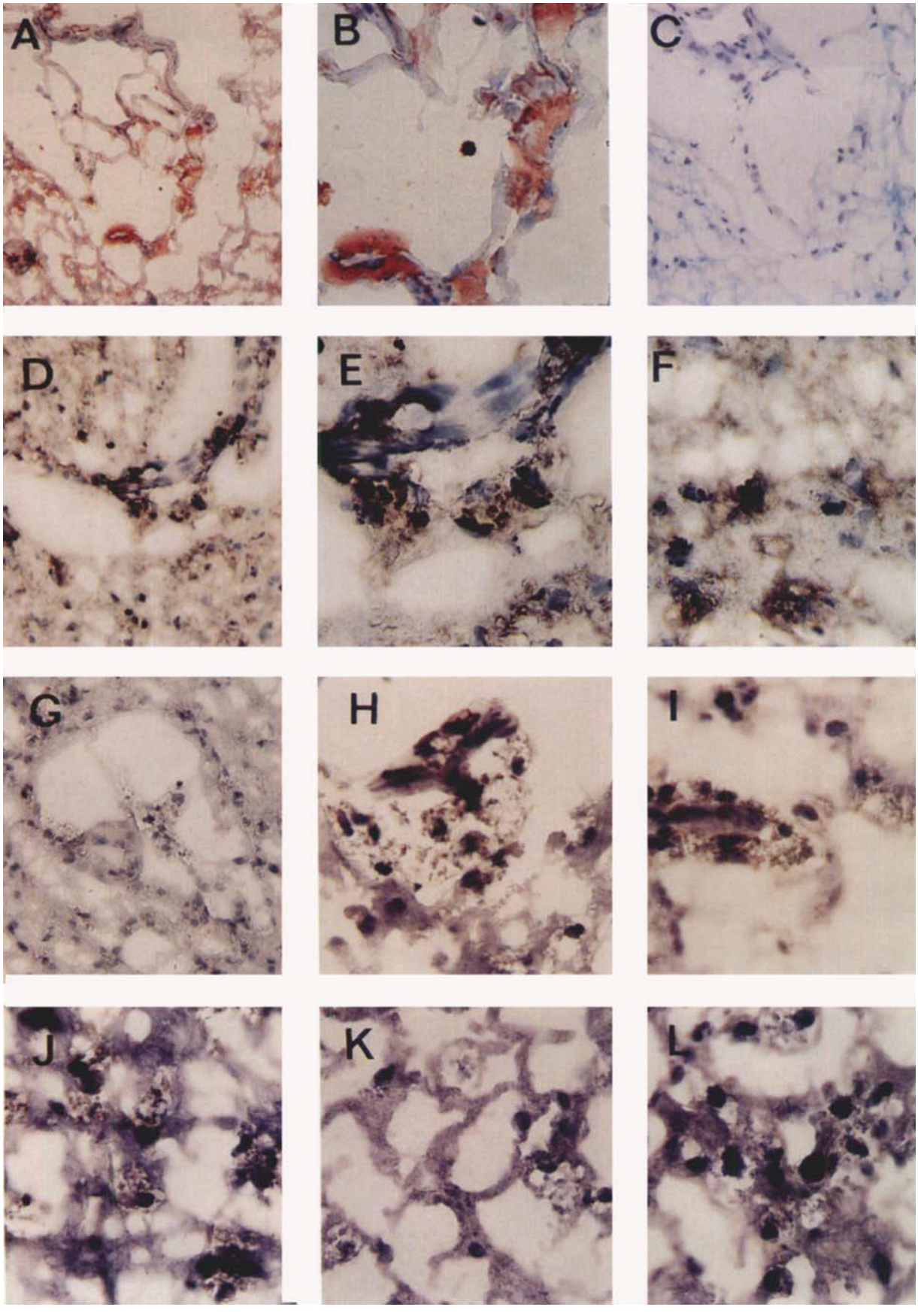
A
B
C
D
E
F
G
H
I
J
K
L

pected, because there is only a 44 nucleotide difference between the N gene coding regions of the two viruses [17]. By in situ hybridization, however, the HCV OC43 probe weakly hybridized to MHV A59–infected cells, whereas the BCV probe did not. The slight degree of sequence divergence between HCV OC43 and BCV may account for this result, but differences in hybridization conditions such as probe concentrations or specific activities may also be responsible for the lack of hybridization of the BCV clone to the tissues and MHV A59–infected cells.

Even in sections that contained viral RNA, there was a paucity of positive cells except in the two patient samples shown in Figures 1 and 2. The low percentage of coronavirus RNA–containing cells is exemplified by the fact that although 52% of the patients with MS were positive, only 11% of the total sections examined were positive (see Results section). This finding may explain the previously reported negative dot-blot hybridization study for HCV OC43 sequences in MS tissue [28]. The dot-blot hybridization technique is considerably less sensitive than in situ hybridization when attempting to detect a very low percentage of positive cells in a total cell population.

In the two patients with rapidly progressive disease, the results from the immunohistochemical screen confirmed those obtained by in situ hybridization because grain development was over similar cells that were antigen-positive. In addition, the possibility that the coronaviruses detected in these human tissue samples have a close relationship to the murine viruses is strengthened because mAb J.3.1 is specific for the N protein of MHV A59 and MHV JHM but not HCV OC43 or HCV 229E [23, 24]. This finding clearly indicates that the 3′ end of the genome is more murine-like. Interestingly, the coronavirus RNA and antigen–positive cells in the two patients with rapidly progressive MS appear to be foamy macrophages, which have a similar appearance to those seen in acute plaques in the rat model of MHV JHM–induced demyelination [29]. Although others have detected viral nucleic acid by in situ hybridization in MS tissue [30], none have reported detecting the corresponding viral antigen. Our study is unique in this regard.

Although coronaviruses are primarily regarded as upper respiratory pathogens, our data show that they are capable of entry into the CNS. It is tempting to hypothesize, based on work done in the murine system [31–33], that human coronaviruses could gain access to the CNS via hematogenous and nonhematogenous routes. Once within the human CNS, coronaviruses may have a role in the induction or maintenance of demyelination, or both, by one or more mechanisms. In our primate studies, we have demonstrated that MHV JHM and the putative MS isolate coronavirus SD can infect, disseminate, and cause demyelination [34]. Studies of coronavirus infection of rodent CNS [9, 12, 35] show that demyelination can be due to direct viral infection and lysis of oligodendrocytes [36]. However, viral persistence in a noncytolytic state appears to be critical to the mechanisms of chronic demyelination [12, 36, 37]; autoimmune reactivity toward CNS proteins may cause demyelination during persistent MHV JHM infection [11, 38]. The potential mechanisms of coronavirus-induced demyelination in humans are currently being tested in our primate model.

Finding coronavirus products in macrophages and monocytes could represent an infection of these cells due to their proximity to the primary infected cell types (i.e., macrophages are infected by extracellular virus or become infected after phagocytosis of other infected cell types). Virus infection of macrophages with subsequent virus spread by the macrophages is known to occur in other coronavirus systems [39]. Whatever the mechanism of macrophage infection, we have confirmed by dual labeling techniques that these cells can be infected in areas of inflammation in the CNS of infected primates (unpublished results). The presence of macrophages in a plaque does not necessarily indicate that viral products will be found; this finding was observed for the two patients shown in Figures 1 and 2. Some plaques containing macrophages contained abundant coronavirus RNA whereas others did not, which implies a timing factor for detection of the viral RNA. This factor was also evident in our primate model of coronavirus demyelination [34], where the immune system cleared detectable virus from some areas while other areas retained viral RNA, antigen, or both. An alternative explanation for finding

Fig 2. Detection of coronavirus antigen in active demyelinating plaques. (A, B) Oil red O stain of section subjacent to section in Figure 1 (H). Note the lipid-laden cells (red color) infiltrating the vascular wall. (C) Luxol-fast blue/periodic acid-Schiff stain of section subjacent to section in A and B. The faint blue stain indicates remaining myelin membranes. Note lack of blue stain in vascular wall where lipid-laden cells were noted in A and B. (D, E) Positive brown horseradish peroxidase reaction product with polyclonal mouse hepatitis virus strain A59 (MHV A59) antisera in foamy cells invading vascular wall and present in surrounding parenchyma. (F) Area adjacent to D and E showing positive brown reaction product in foamy cells. (G) In patient studied in Figure 1 A–G, a blood vessel leaving primary antibody out of reaction. Note absence of reaction product. (H, I) Subjacent section to (G) demonstrating positive reaction product in foamy cells surrounding the vascular wall; primary antibody was mAb J.3.1. (J, K, L) Positive foamy cells in active demyelinating lesion stained with mAb J.3.1. In (K) the antibody was left out, and in (L) the section was pretreated with polyclonal MHV A59 rabbit antisera and processed as in (J). Note the lack of reaction product in K and L. (A, C, D, and G ×400; B, E, F, H–L ×800.)

coronavirus RNA and antigen in macrophages is that these cells can be nonspecifically sequestered in the CNS after a systemic infection; this mechanism is currently under investigation in a prospective study of patients with MS and in the primate system.

This study indicates that coronaviruses with similarities to murine coronaviruses are capable of infecting humans and thus may represent a previously unidentified human pathogen. The data presented herein do not establish coronavirus as an etiological agent for MS, but they do indicate that coronaviruses are present in the human CNS and are preferentially detected in MS tissue. Possibly, coronaviruses are not involved in pathogenesis; perhaps patients with MS are merely susceptible to CNS infection after onset of the disease. However, in light of the data on coronavirus-induced demyelination in rodents and the demonstration that coronaviruses induce encephalomyelitis and demyelination in primates [34, 40], it is unlikely that coronaviruses would be present in human CNS purely as a nonpathogenic infection. Further studies are required before attributing a definite role for this pathogen in the MS disease process.

This work was supported by grants from the Swedish Medical Foundation, the Fausel Foundation, and the Writer family. The Rocky Mountain MS Center Tissue bank is supported by grant #RG-2108-B-5 from the National Multiple Sclerosis Society.

Monoclonal J.3.1 was kindly provided by J. O. Fleming, MD. Cloned probes for OC43 and 229E were kindly provided by M. M. Lai, PhD. Cloned MHV A59 probe was a gift from J. Leibowitz, MD, PhD and S. Weiss, PhD. P. Lollar assisted with manuscript preparation.

References

1. Kurtzke JF. Epidemiologic contributions to multiple sclerosis: an overview. Neurology 1980;30:61–79
2. Kurtzke JF, Hyllested K. Multiple sclerosis in the Faroe Islands. I. Clinical and epidemiological features. Ann Neurol 1979; 5:6–21
3. Elian M, Nightingale S, Dean G. Multiple sclerosis among United Kingdom-born children of immigrants from the Indian subcontinent, Africa and the West Indies. J Neurol Neurosurg Psychiatry 1990;53:906–911
4. Booss J, Kim JH. Evidence for a viral etiology of multiple sclerosis. In: Cook SD, ed, Handbook of multiple sclerosis. New York: Marcel Dekker, 1990:41–61
5. Cabirac GC, Ries D, Murray RS. Multiple sclerosis, human T-lymphotropic virus type I, and human endogenous retrovirus sequences. Ann Neurol 1991;29:343–344
6. Ehrlich GD, Glaser JB, Bryz-Gornia V, et al. Multiple sclerosis, retroviruses, and PCR. Neurology 1991;41:335–343
7. Burks JS, DeVald BL, Jankovsky LD, Gerdes JC. Two coronaviruses isolated from central nervous system tissue of two multiple sclerosis patients. Science 1980;209:933–934
8. Tanaka R, Iwasaki Y, Koprowski H. Ultrastructural studies of perivascular cuffing cells in multiple sclerosis brain. J Neurol Sci 1976;28:121–126
9. Weiner LP. Pathogenesis of demyelination induced by a mouse hepatitis virus (JHM virus). Arch Neurol 1973;28:298–303
10. Kyuwa S, Yamaguchi K, Toyoda Y, Fujiwara K. Induction of self-reactive T cells after murine coronavirus infection. Virology 1991;65:1789–1795
11. Watanabe R, Wege H, Meulen ter V. Adoptive transfer of EAE-like lesions from rats with coronavirus induced demyelinating encephalomyelitis. Nature 1983;305:150–153
12. Mendelman PM, Jankovsky LD, Murray RS, et al. Pathogenesis of coronavirus SD in mice. I. Prominent demyelination in the absence of infectious virus production. Arch Neurol 1983;40: 493–498
13. Stroop WG, Brahic M, Baringer JR. Detection of tissue culture-adapted Theiler's virus RNA in spinal cord white matter cells throughout infection. Infect Immunity 1982;37:763–770
14. Vafai A, Murray RS, Wellish M, et al. Expression of varicella-zoster and herpes simplex virus in normal human trigeminal ganglia. Proc Natl Acad Sci USA 1988;85:2362–2366
15. Budzilowicz CJ, Wilczynski SP, Weiss SR. Three intergenic regions of coronavirus mouse hepatitis virus strain A59 genome RNA contain a common nucleotide sequence that is homologous to the 3′ end of the viral mRNA leader sequence. Virology 1985;53:834–840
16. Schreiber SS, Kamahora T, Lai MMC. Sequence analysis of the nucleocapsid protein gene of human coronavirus 229E. Virology 1989;169:141–151
17. Kamahora T, Soe LH, Lai MMC. Sequence analysis of nucleocapsid gene and leader RNA of human coronavirus OC43. Virus Res 1989;12:1–9
18. Lapps W, Hogue BG, Brian DA. Sequence analysis of the bovine coronavirus nucleocapsid and matrix protein genes. Virology 1987;157:47–57
19. Kapke PA, Brian DA. Sequence analysis of the porcine transmissible gastroenteritis coronavirus nucleocapsid protein gene. Virology 1986;151:41–49
20. Everett RD. A detailed mutational analysis of Vmw110, a trans-acting transcriptional activator encoded by herpes simplex virus type 1. EMBO J 1987;6:2069–2076
21. Feinberg AP, Vogelstein B. A technique for radiolabeling restriction endonuclease fragments to high specific activity. Anal Biochem 1983;132:6–13
22. Gerdes JC, Klein I, DeVald BL, Burks JS. Coronavirus isolates SK and SD from multiple sclerosis patients are serologically related to murine coronaviruses A59 and JHM and human coronavirus OC43; but not to human coronavirus 229E. J Virol 1981;38:231–238
23. Fleming JO, Zaatari FAK, Gilmore W, et al. Antigenic assessment of coronaviruses isolated from patients with multiple sclerosis. Arch Neurol 1988;45:629–633
24. Taguchi F, Fleming JO. Comparison of six different murine coronavirus JHM variants by monoclonal antibodies against the E2 glycoprotein. Virology 1989;169:233–235
25. Malkova D, Holubova J, Kolman JM, et al. Isolation of tettnang coronavirus from man. Acta Virol (Prague) 1980;24:363–366
26. Fazzini E, Fleming J, Fahn S. Cerebrospinal fluid antibodies to coronaviruses in patients with parkinson's disease. Neurology 1990;40(suppl 1):169
27. Weiss SR. Coronaviruses SD and SK share extensive nucleotide homology with murine coronavirus MHV-A59, more than that shared between human and murine coronavirus. Virology 1983;126:669–677
28. Sorenson O, Collins A, Flintoff W, et al. Probing for the human coronavirus OC43 in multiple sclerosis. Neurology 1986; 36:1604–1606
29. Watanabe R, Wege H, Meulen Ter V. Comparative analysis of coronavirus JHM-induced demyelinating encephalomyelitis in Lewis and brown Norway rats. Lab Invest 1987;57:375–390
30. Haase AT, Ventura P, Gibbs CJ, Tourtellotte WW. Measles

virus nucleotide sequences: detection by hybridization in situ. Science 1981;212:672–675
31. Perlman S, Jacobsen G, Afifi A. Spread of a neurotropic murine coronavirus into the CNS via the trigeminal and olfactory nerves. Virology 1989;170:556–560
32. Perlman S, Evans G, Afifi A. Effect of olfactory bulb ablation on spread of a neurotropic coronavirus into the mouse brain. J Exp Med 1990;172:1127–1132
33. Lavi E, Fishman PS, Highkin MK, Weiss SR. Limbic encephalitis after inhalation of a murine coronavirus. Lab Invest 1988;58: 31–36
34. Murray RS, Cai G-Y, Hoel K, et al. Coronavirus infects and causes demyelination in primate central nervous system. Virology 1992 (in press)
35. Lavi E, Gilden DH, Wroblewska Z, et al. Experimental demyelination produced by the A59 strain of mouse hepatitis virus. Neurology 1984;34:597–603
36. Dubois-Dalcq ME, Doller EW, Haspel MV, et al. Cell tropism and expression of mouse hepatitis viruses (MHV) in mouse spinal cord cultures. Virology 1982;119:317–331
37. Lavi E, Gilden DH, Highkin MK, Weiss SR. Persistence of mouse hepatitis virus A59 RNA in a slow virus demyelinating infection in mice as detected by *in situ* hybridization. J Virol 1984;51:563–566
38. Cross AH, McCarron R, McFarlin DE, Raine CS. Adoptively transferred acute and chronic relapsing autoimmune encephalomyelitis in the PL/J mouse and observations on altered pathology by intercurrent virus infection. Lab Invest 1987;57:499–512
39. Weiss RC, Scott FW. Pathogenesis of feline infectious peritonitis: pathologic changes and immunofluorescence. Am J Vet Res 1981;42:2036–2048
40. Kersting GE, Pette E. Zur pathohistologie und pathogenese der experimentellen JHM-Virusencephalomyelitis des affen eingegangen. Deutsche Zeitschrift f. Nervenheilkunde 1956;174: 283–304